Hindawi
Scientific Programming
Volume 2021, Article ID 6662097, 10 pages
https://doi.org/10.1155/2021/6662097

Research Article

Monitoring, Analyzing, and Modeling for Single Subsidence Basin in Coal Mining Areas Based on SAR Interferometry with L-Band Data

Zhiyong Wang,[1] **Jingzhao Zhang**,[1,2] **Yaran Yu**,[1] **Jian Liu**,[1] **Wei Liu**,[1] **Na Jiang**,[3] **and Donge Guo**[3]

[1]*College of Geodesy and Geomatics, Shandong University of Science and Technology, Qingdao 266590, China*
[2]*Shandong Institute of Geological Surveying and Mapping, Jinan 250011, China*
[3]*Shandong Institute of Land Surveying and Mapping, Jinan 250013, China*

Correspondence should be addressed to Jingzhao Zhang; 564158441@qq.com

Received 16 December 2020; Revised 15 January 2021; Accepted 24 January 2021; Published 9 February 2021

Academic Editor: Habib Ullah Khan

Excessive exploitation of underground mine resources has caused serious land subsidence in China. This paper focused on monitoring and modeling the single subsidence basin in coal mining area based on SAR interferometry (InSAR). The optimum InSAR processing strategy to monitor the mining subsidence was built to obtain the land subsidence with large deformation. And a method of three-dimensional mathematical modeling of single subsidence basin based on InSAR measurements was presented. Using Jining Coalfield (China) as the study area, we acquired 7 L-band PALSAR images from January 2008 to February 2010 to monitor the land subsidence in Jining Coalfield. The deformation maps in Jining Coalfield in different periods were obtained. Taking the Geting Coal Mine within the Jining coalfield as an example, we finely analyzed and interpreted the deformation maps. Compared with the simultaneous filed measurements, the precision of deformation measurement using D-InSAR in mining area was analyzed. The root mean square error was 1.37 cm. The method of fine interpretation and analysis for a single subsidence basin was established. The experiments have proved that InSAR technique with L-band InSAR data is suitable for monitoring mining subsidence with large deformation. And the 3D mathematical modeling method could be used for the single subsidence basin in coal mining area.

1. Introduction

Monitoring the land subsidence over mining regions is one of the most important tasks in monitoring the geographical conditions. Excessive exploitation of underground mine resources has caused serious land subsidence and ruined farmland and some water pit collapse in China [1, 2]. It has become one of the most serious problems in restricting the environmental, social, and economic sustainable development in coal mining area. So, it is urgent to obtain the information about the land subsidence in coal mining area. The traditional monitoring methods mainly include the leveling, Global Positioning System (GPS), and total station [2, 3]. These methods have some limitations such as needing much field work, being time consuming and laborious, and having high cost [1], and the observation points are difficult to preserve. In addition, the update period is too long and the measuring data is discrete. So, we should seek a new monitoring method with low cost, short production period, and continuous data in monitoring the land subsidence over mining regions.

The space-borne Interferometric Synthetic Aperture Radar (InSAR) is a new technique for Earth observation in the late 1900s [4–7]. It provides a new method to monitor the Earth surface deformation. It can quickly get the large-area surface deformation with high precision. And InSAR can identify some previously unknown land subsidence areas. It has been turned out to be an effective technique for

land subsidence measurement due to its precision, spatial coverage, and resolution [8, 9]. The capability of InSAR for surface deformation mapping has been demonstrated in many applications, such as earthquake activity [10], volcanic activity [11, 12], the land subsidence in the city caused by groundwater over exploitation [13, 14], landslide [15], and glacier movement [16].

InSAR technique has been applied to monitor the land subsidence in coal mining area [17–30]. Ji et al. [18] demonstrated InSAR's ability to cost-effectively monitor illegal mining activities. A DInSAR-based illegal-mining detection system (DIMDS) was proposed to exploit the geometric, spatial, and temporal characteristics of those subsidence patterns [19]. Zheng et al. [20] analyzed land subsidence induced by coal mining in a 200 km^2 area in the Ordos Basin for the time period 2006–2015 using SBAS InSAR and D-InSAR. Hayman et al. [21] investigated the performance of the three satellite missions (Radarsat-2, Sentinel-1, and ALOS-2) with different imaging modes for mapping longwall mine subsidence. Yang et al. [22] presented a novel space-based method for locating and defining the underground goaf caused by coal extraction using Interferometric Synthetic Aperture Radar (InSAR) techniques. Xia and Wang [23] proposed a method that relied on the principle of the probability integration method (PIM) and on synthetic aperture radar interferometry (InSAR) to retrieve the location of an underground goaf. Du et al. [24] proposed a feature-points-based method for the efficient location of mining goafs based on D-InSAR. Chen et al. [25] employed the small baseline subset interferometry synthetic aperture radar (SBAS-InSAR) technology to obtain the time-series residual surface deformation based on the 40 Sentinel-1A images acquired from 14th February 2017 to 17th May 2020.

Although InSAR technique has been applied to monitor the land subsidence over mining regions, the special surface environment in mining area and the characteristics of mining subsidence restrict the application of InSAR technique in coal mining area on a large scale. There have been some problems and difficulties in monitoring the land subsidence in mine area. For example, too large deformation will exceed the maximum deformation gradient [31] that InSAR can measure; the coherence caused by high vegetation land cover is poor; and the reliability and accuracy of InSAR monitoring are low. These increase the difficulty in monitoring the land subsidence with InSAR technique.

According to the problems about obtaining the mining subsidence information, we carried out some studies to obtain the land subsidence based on InSAR technique. We will explore a suitable and feasible method and technical process related to the InSAR data processing. In this paper, the major objective is to provide an effective solution to obtain accurate and critical information on the land subsidence in coal mining area.

This paper is organized as follows. The study area and SAR data are presented in Section 2. Section 3 describes the method and data processing strategy for monitoring the surface deformation with InSAR technique. And a method of three-dimensional mathematical modeling of subsidence basin based on InSAR measurements is presented. In Section 4, taking the Jining Coalfield (China) as study area, we obtain the land subsidence using InSAR technique with PALSAR data. And we analyze and interpret the results of mining subsidence based on InSAR technique. Finally, some valuable conclusions drawn from this study are given in Section 5.

2. Data and Materials

2.1. Study Area. The study area is located in the Jining City, which is the west-south part of the Shandong Province, North China. The region extends from 116.36°E to 116.94°E and from 35.32°N to 35.54°N (see Figure 1). There have been more than 20 coal mines, such as Liangbaosi Coal Mine, Geting Coal Mine, Tangkou Coal Mine, Daizhuang Coal Mine, Xuchang Coal Mine, Nantun Coal Mine, Dongtan Coal Mine, and Gucheng Coal Mine. It caused serious surface collapse because of long-term and high-intensitive coal mining.

2.2. Data. In order to monitor the mining-induced land subsidence with large deformation in coal mining area, the ALOS PALSAR data, which are L band (the wavelength is 23.6 cm), were used. Its central frequency is 1270 MHz. This means it has greater penetration.

We used a total of 7 L-band ALOS PALSAR images acquired from January 2008 to February 2010 over the Jining coalfield from an ascending orbit, as listed in Table 1. All PALSAR data were Fine Beam Single Polarization (FBS) imaging mode (single-look complex images, CEOS (Committee for Earth Observing Satellites) standard format and Level 1.1 products) and in HH polarization with the 34.3° incidence angle. The ALOS PALSAR data has a swath of about 70 km and a spatial resolution of about 7 m. The satellite repeat period of ALOS is 46 days.

From the optical remote sensing image, we can see that there are mostly farmlands in the study area and the vegetation is rich and well grown. This increases the difficulty in monitoring the land subsidence with InSAR technique.

In addition, the SRTM DEM in this region was used to remove the flat Earth phase in InSAR data processing and to geocode some products. It can also be used to do SAR simulating processing to remove the phase due to the topography [6, 7, 26].

3. Methods

SAR interferometry can provide the mining subsidence information and spatial-temporal evolution about the surface deformation based on time series radar data. The following is a brief introduction of the basic principle and process of InSAR about monitoring the mining deformation.

3.1. The Basic Principle for Monitoring the Land Subsidence Using InSAR Technique. In fact, the phase of interferogram consists of 5 parts as follows [6, 7]:

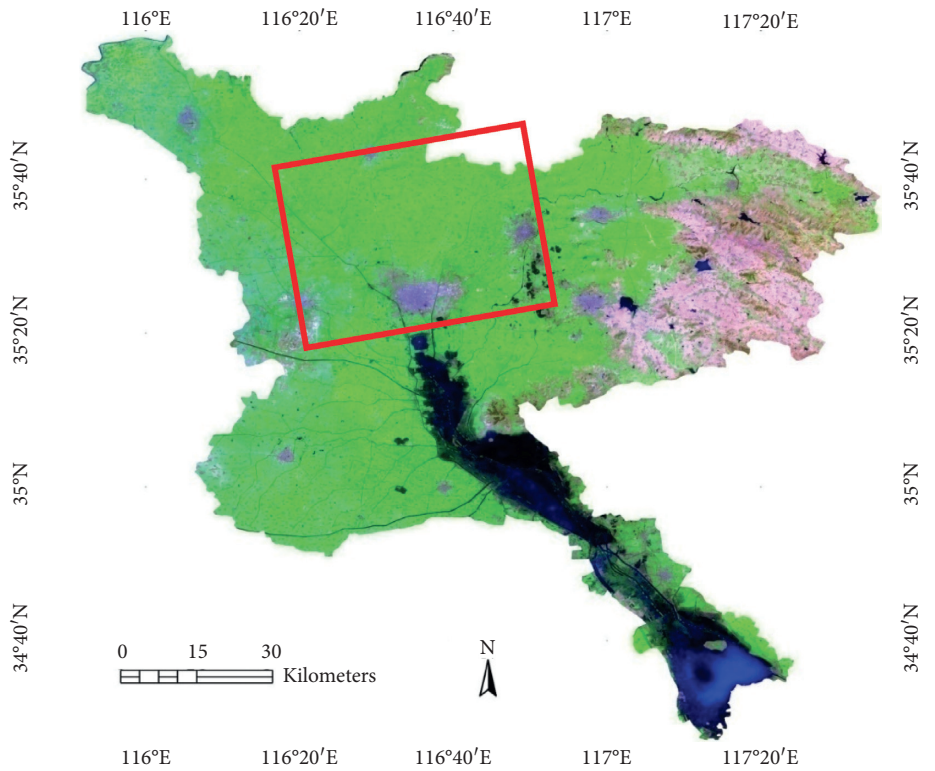

Figure 1: The location of the Jining coalfield is shown. The coverage of SAR data in Jining coalfield, Shandong province, China, is shown. The base map is the mosaic image product of Jining district from multiple Landsat5 TM data from September 2005 to March 2007. The red box is the coverage of PALSAR (path: 449, frame: 700).

Table 1: The SAR data used in this study.

No.	Sensor	Acquisition date	Orbit	Path/track	Frame	Incidence angle (°)
1	PALSAR	08/01/2008*	10,423	449	700	34.3
2	PALSAR	23/02/2008	11,094	449	700	34.3
3	PALSAR	09/04/2008	11,765	449	700	34.3
4	PALSAR	10/01/2009	15,791	449	700	34.3
5	PALSAR	25/02/2009	16,462	449	700	34.3
6	PALSAR	13/01/2010	21,159	449	700	34.3
7	PALSAR	28/02/2010	21,830	449	700	34.3

*date/month/year.

$$\varphi_{\text{int}} = \varphi_{\text{topography}} + \varphi_{\text{displacement}} + \varphi_{\text{atmosphere}} + \varphi_{\text{flat}} + \varphi_{\text{noise}}, \quad (1)$$

where $\varphi_{\text{topography}}$ is the phase due to the topography; $\varphi_{\text{displacement}}$ is the phase due to the surface deformation at line of sight (LOS) of radar; $\varphi_{\text{atmosphere}}$ is the phase due to the atmospheric effects; φ_{flat} is the flat Earth phase due to the special imaging geometry, side looking imaging; φ_{noise} is the phase noises from the speckle due to coherence imaging, system noise, and radar shadow.

For monitoring the surface deformation with InSAR technique, there are three methods, named as two-pass method, three-pass method, and four-pass method [4, 6, 7, 10]. The basic principle of InSAR can be found in the literatures [6, 7, 10]. Two-pass approach differential interferometry is more suitable for monitoring the land subsidence with large deformation [23, 26]. It needs two sets of radar data acquired from the similar orbit and the DEM with high precision.

3.2. The Optimum InSAR Processing Strategy to Monitor the Mining Subsidence. The procedures of two-pass D-InSAR include the interferogram generation, the SAR simulation based on DEM, the differential processing between the real interferogram and the simulated interferogram, the phase unwrapping, the transformation from the phase to deformation, the geocoding, and so on [6, 7]. The methods and flowchart of data processing can be seen in [6, 7, 10]. Figure 2 is the technical flowchart for monitoring the mining subsidence with InSAR technique in our study.

When the coherence of InSAR pair is low, for example, in the densely vegetated area, a prefilter (including the

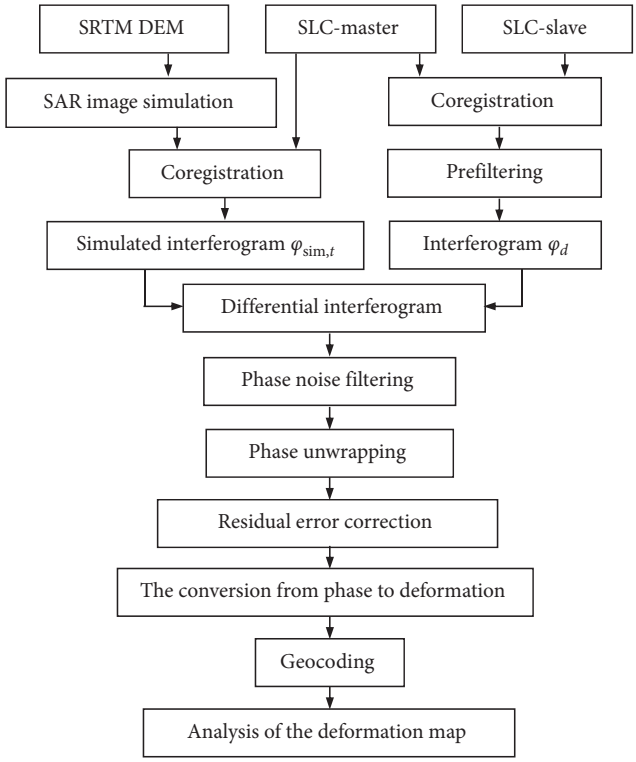

Figure 2: The block diagram of the approach implemented in our study.

spectral shift filter and Doppler filter) is necessary in InSAR data processing [6]. The spectra of master and slave acquisitions are not completely overlapping. The spectral shift filter is intended to remove the part of the master and slave spectra which are not overlapping. The Doppler filter can remove the portion of the azimuth spectra, which are not common between master and slave image. The prefilter can obviously improve the coherence of interferogram and therefore improve the reliability and accuracy of InSAR measuring.

In addition, we also proposed an optimum strategy from coarseness to fine in InSAR processing. The specific method was as follows. Firstly, it carries out the coarse differential interferometric processing for the whole image. The number of looks in range direction was selected bigger in multilooking processing now. For example, the multilook of ALOS PALSAR data is 4 : 10 in the range direction and azimuth direction, respectively. The differential interferogram should not carry out the subsequent data processing, such as the phase unwrapping and the transformation from phase to deformation. We can find several settlement regions according to the differential interferogram. Then, we subset the radar data to several parts according to the locations of settlement regions, which include one or two coal mines. At last, it carries out the fine differential interferometric processing and subsequent data processing for every part. The number of looks in the range direction should be as small as possible in multilooking processing now. For example, the multilook of ALOS PALSAR data is 1 : 2 in the range direction and azimuth direction, respectively. This strategy can not only accelerate the speed of data processing, but also ensure the accuracy of monitoring results. Especially for the phase unwrapping, it can obtain more reliable result in small region.

3.3. The Method of Three-Dimensional Modeling for Subsidence Basin Based on InSAR Measurements. After underground coal mining, a series of subsidence basins will form in the mining area. Based on analyzing a large number of interferograms using SAR interferometry in coal mine area, we found that they are usually manifested as a series of concentric circles or concentric ellipses with similar shapes for the single subsidence basin in the InSAR interferograms [32]. In order to conduct quantitative analysis of single subsidence basin, the InSAR monitoring results can be used to establish the mathematical model of the single subsidence basin. Through a series of experimental verifications, especially the analysis of the morphology of the horizontal section and vertical section of the subsidence basin, the mathematical model of the subsidence basin in the mining area can be established:

$$h = -ae^{-\left(\left(\left(x-x_0\right)^2\right)/b^2\right)+\left(\left(\left(y-y_0\right)^2\right)/c^2\right)}, \quad (2)$$

where h is the settlement; (x, y) is the plane coordinates of settlement points; (x_0, y_0) is the position of maximum subsidence center; a is the influence of the subsidence factor; b and c are the semimajor axis and semiminor axis of an elliptic equation, respectively. That is to say, 5 parameters of the mathematical model should be needed to solve: x_0, y_0, a, b, c. The parameters x_0 and y_0 determine subsidence basin the location of the maximum settlement. The parameter a determines the size of the ground settlement shape. The parameters b and c determine the geometric shapes of subsidence basin. These five parameters will determine the position and form of subsidence basin in space.

Parameter a is obtained directly according to the maximum settlement amount of the subsidence basin monitored by InSAR. Parameters x_0 and y_0 are determined by the position of the maximum settlement amount of the subsidence basin. The maximum settlement amount and its position are detected and recorded through two-dimensional search in the deformation map. The other two parameters, b and c, determine the shape of the ellipse. And the solutions can be obtained by means of least square fitting based on some InSAR measurements at settlement points.

4. Results and Discussion

4.1. The Differential Interferogram in Jining Coalfield. In order to monitor the land subsidence in Jining coalfield in detail, we carried out the differential InSAR processing for the 7 PALSAR radar data. We built 6 optimum interferometric pairs according to the parameters of the time of data acquisition and the baselines. The information about the InSAR pairs can be seen in Table 2.

We carried out the interferometric data processing for all InSAR pairs according to the processing flowchart in Figure 2. The InSAR complex data registration adopted the

Table 2: The information about compositions and baselines of interferometric pairs.

No.	InSAR pair	Temporal baseline (d)	Perpendicular baseline $B_\perp$ (m)	Parallel baseline $B_\parallel$ (m)
1	08/01/2008–23/02/2008	46	679.3	294.6
2	23/02/2008–09/04/2008	46	443.4	397.5
3	09/04/2008–10/01/2009	6 * 46	−3914.2	−2833.0
4	10/01/2009–25/02/2009	46	194.9	154.8
5	25/02/2009–13/02/2010	7 * 46	1713.3	1216.4
6	13/02/2010–28/02/2010	46	604.1	451.1

automatic search technique based on window. The phase noise was filtered using the modified Goldstein Radar Interferogram Filter [33, 34]. The phase unwrapping process becomes difficult due to the presence of large areas of low coherence. In this case, the minimum cost flow (MCF) algorithm [35] enables obtaining better results than other methods. The ratio of multilooking is 1 : 2. The pixel size in range direction is 7.49 m, and the pixel size in azimuth direction is 6.15 m for the differential interferograms. It is necessary to carry out the processing of resampling because the pixel size is not the same in range direction and in azimuth direction. In order to further analyze the subsidence of deformation map, geocoding the differential interferograms is in need. They are the results of geocoded differential interferograms as shown in Figure 3.

4.2. The Mining-Induced Land Deformation Fields in Jining CoalField. Then, we can obtain the land deformation maps for every InSAR pairs after the conversion from the phase to deformation. The deformation maps have carried out some data processing procedures, such as the residual phase correction, the conversion from phase to deformation, and geocoding the products. They have absolute geographical coordinates. According to the amount of deformation, the settlement is classified with different colors (see Figure 4).

Through experiment, we also found that the InSAR pairs with too long interval or with too long perpendicular baseline cannot generate distinct interferometric fringes.

We also calculated the area of the land subsidence for the several important coal mines in different time intervals. They include Liaobaosi Coal Mine, Geting Coal Mine, Yunhe Coal Mine, Tangkou Coal Mine, and Daizhuang Coal Mine. The areas of land subsidence are listed in Table 3. From Table 3, we can find that the land subsidence is very serious due to excessive exploitation of underground mine resources. The land subsidence of these 6 coal mines within Jining coalfield exceeds 6 km^2.

A magnitude of 94.4 cm was firstly monitored by L-band InSAR in Jining coalfield. It appeared around the Dongtan Coal Mine in time interval from 10th January to 25th February, 2009. The radius of this subsidence basin is about 350 m and the major influence radius of this subsidence basin is about 256 m.

4.3. Accuracy Verification. In order to verify and evaluate the accuracy of settlement monitoring in InSAR mining area, precise leveling observation was carried out simultaneously in the study area.

The comparison of monitoring results between InSAR technique and leveling is shown in Figure 5. According to Figure 5, the deformation trend of InSAR monitoring results and leveling monitoring results is basically consistent, and the root mean square error was 1.37 cm. The root mean square error was relatively large. This was mainly caused by the inconsistency of observation time and space. Firstly, the time period of InSAR technique and leveling monitoring was not completely consistent. The time period of InSAR monitoring was from 13th January to 28th February, 2010, while the time period of leveling was from 11th January to 26th February, 2010. They were not completely consistent. Secondly, leveling observation monitors the deformation information on a "point," while InSAR technique deals with the deformation information on a "surface" (i.e., pixel). In fact, it is the comparison between "point" and "surface," so they cannot correspond exactly.

4.4. Fine Analysis and Interpretation for Single Subsidence Basin. It is very important to analyze the subsidence conditions of single coal mine. In the following, we take the interferometric pair with the time interval from 8th January to 23rd February, 2008 in Geting Coal Mine within Jining coalfield as an example to illustrate the fine analysis for the mining subsidence. We can generate the geocoded deformation map, the deformation contours, the subsidence profile, and three-dimensional deformation map for the single coal mine. Figure 6 is the results of fine analysis for single coal mine, taking the Geting Coal Mine as an example. Then, the subsidence area can be counted based on the deformation map. Table 4 is the statistics of subsidence area of Geting Coal Mine.

The maximum land subsidence in this time interval is 39.3 cm. The area which the settlement exceeds 5 cm reached 0.24 km^2. And the remaining settlement areas statistics are shown in Table 4.

4.5. Modeling of Subsidence Basin Based on InSAR Measurements. Taking Geting Coal Mine as an example, 46 points are selected to participate in the calculation. And the fitting model parameters can be obtained by calculating according to the least square method. In the image coordinate system, $b = 36.13$ and $c = 34.17$.

Thus, the three-dimensional model of the subsidence basin of Geting Coal Mine can be established as follows:

$$h = -0.393e^{-\left(\left((x-175)^2/36.13^2\right)+\left((y-159)^2/34.17^2\right)\right)}. \quad (3)$$

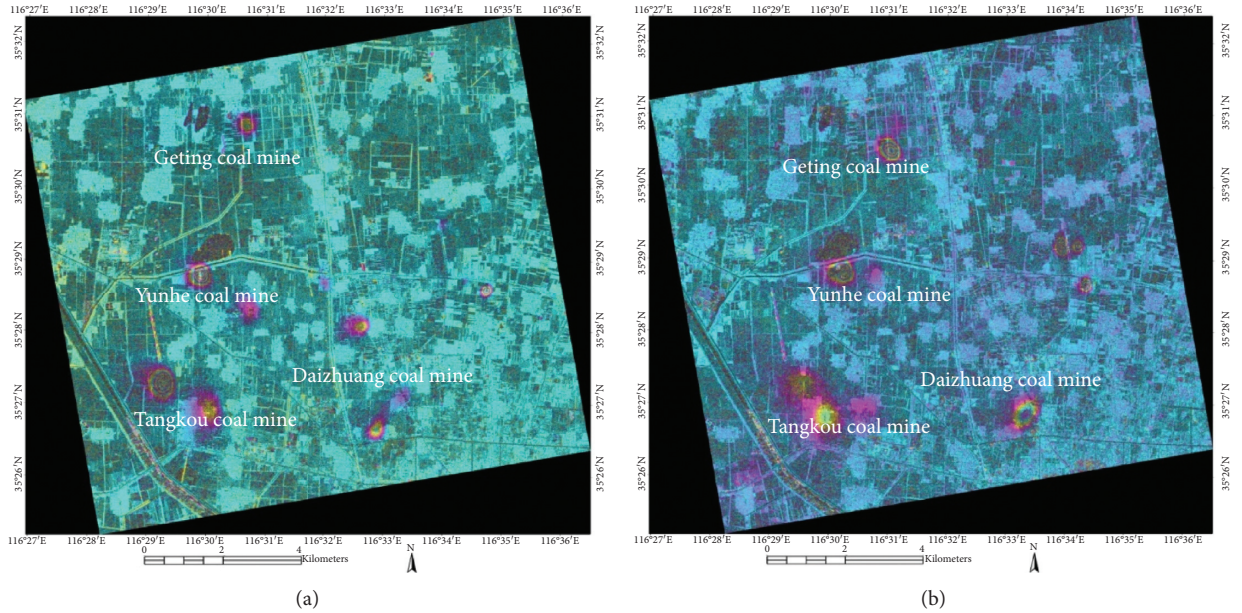

Figure 3: The geocoded differential interferogram in experimentation area. Two of the differential interferograms are only shown here. There are several distinct settlement regions in the differential interferograms. They are Geting Coal Mine, Yunhe Coal Mine, Tangkou Coal Mine, Daizhuang Coal Mine, and Xuchang Coal Mine. (a) is the geocoded differential interferogram in time interval from 8th January to 23rd February 2008; (b) is the geocoded differential interferogram in time interval from 10th January to 25th February, 2009.

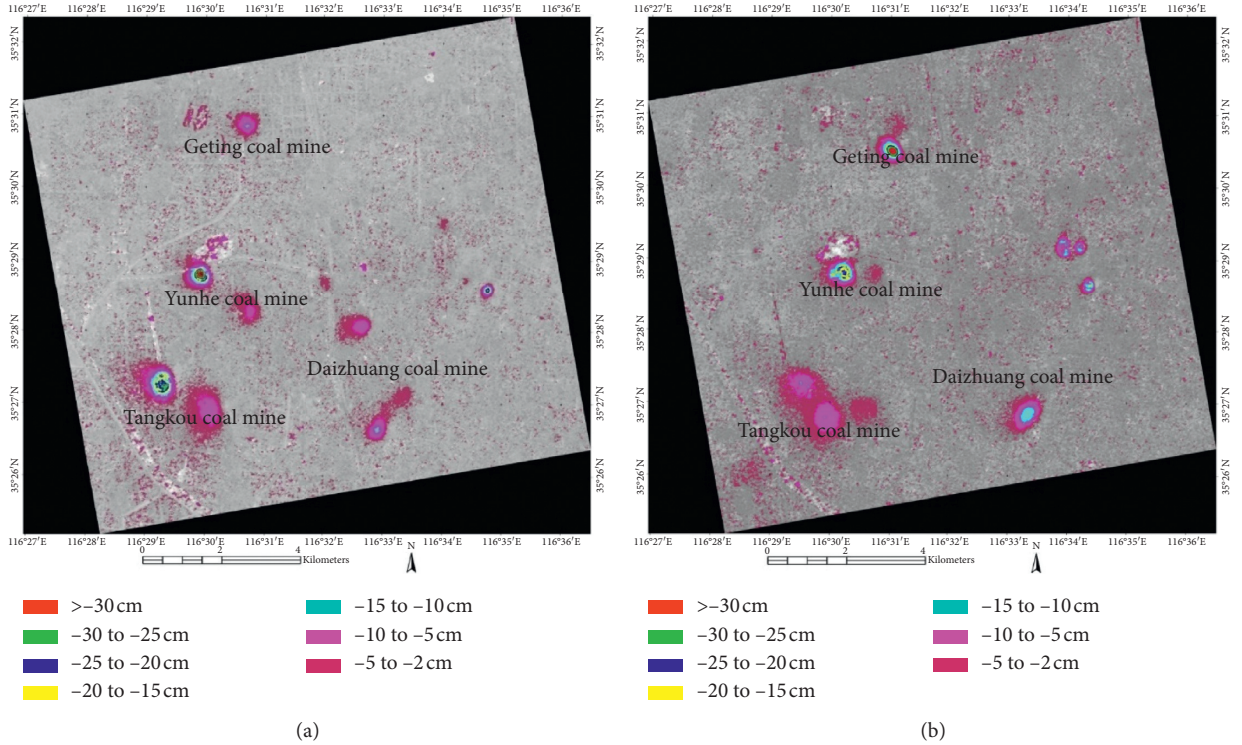

Figure 4: The deformation maps in Jining coalfield in two periods. (a) is the deformation map in time interval from 8th January to 23rd February, 2008; (b) is the deformation map in time interval from 10th January to 25th February, 2009.

In view of the transformation of image coordinate system to geographic coordinate system, pixel size and geographic coordinate system need to be considered.

Figure 7 is the 3D display of the established model. From Figure 7, it can be seen that the 3D model is very consistent with the subsidence basin monitored by InSAR. Therefore,

Table 3: The area statistics of the land subsidence of several important coal mines within Jining coalfield.

Coal Mine	The area of land subsidence (km^2)			
	08/01/2008–23/02/2008	23/02/2008–09/04/2008	10/01/2009–25/02/2009	13/01/2010–28/02/2010
Liaobaosi Coal Mine	0.672	0.778	0.868	0.418
Geting Coal Mine	0.187	0.070	0.416	0.209
Yunhe Coal Mine	0.360	0.227	0.503	—
Tangkou Coal Mine	0.755	0.902	1.757	1.664
Daizhuang Coal Mine	0.299	0.315	0.572	0.468
Dongtan Coal Mine	0.882	0.752	1.871	1.564

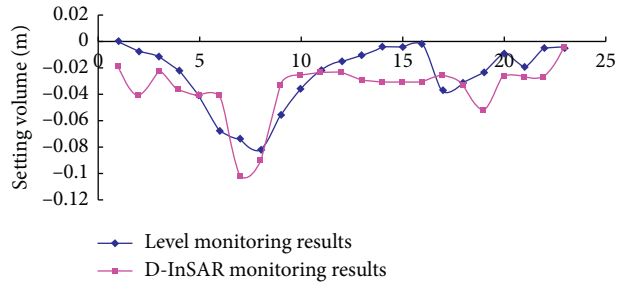

Figure 5: Comparison of monitoring results between D-InSAR and leveling.

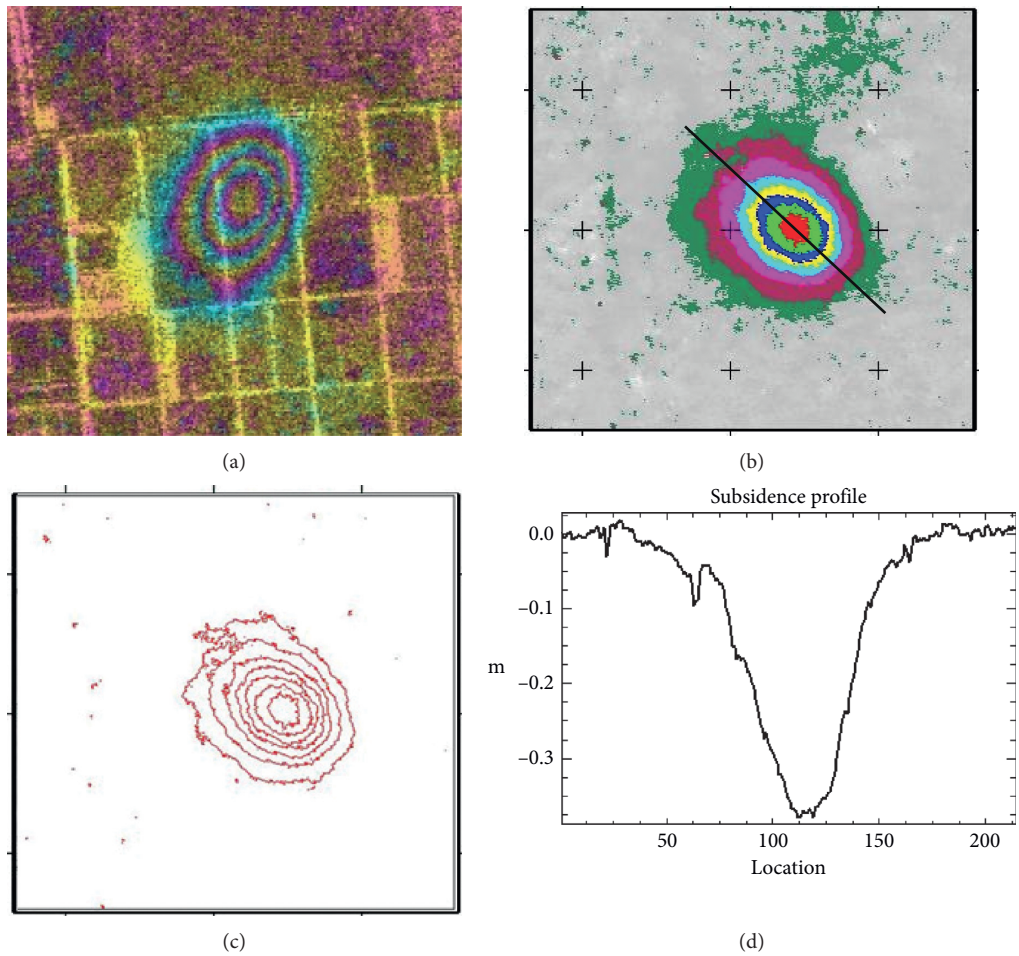

Figure 6: The fine analysis and interpretation for the deformation map in Geting Coal Mine in the interval from 10th January to 25th February, 2010. (a) is the original differential interferogram over the Geting Coal Mine in range direction and azimuth direction coordinate system. It has carried out the interferometric processing, removal of the flat-earth phase, and phase filtering. There are 3 fringes in the interferogram. That is to say, the maximum subsidence is about 35 cm. (b) is the geocoded deformation map in the Geting Coal Mine. It has carried out the phase unwrapping, the conversion from the deformation phase to land subsidence, and geocoding. The UTM (Universal Transverse Mercator) projection is selected in the map projection processing. The pixel size of geocoded map is 5 m. (c) The deformation contours in the Geting Coal Mine are shown. The deformation contours from outer to inner are −2 cm, −5 cm, −10 cm, −15 cm, −20 cm, −25 cm, and −30 cm, respectively. (d) The subsidence profile along the coal mining working face is shown.

Table 4: The area statistics of the land subsidence in Geting Coal Mine (10/01/2009–25/02/2009).

Land subsidence	>5 cm	>10 cm	>15 cm	>20 cm	>25 cm	>30 cm	>35 cm	>40 cm
Pixels	9,549	5,863	3,772	2,586	1,746	1,012	348	0
Area (m^2)	238,725	146,575	94,300	64,650	43,650	25,300	8,700	0

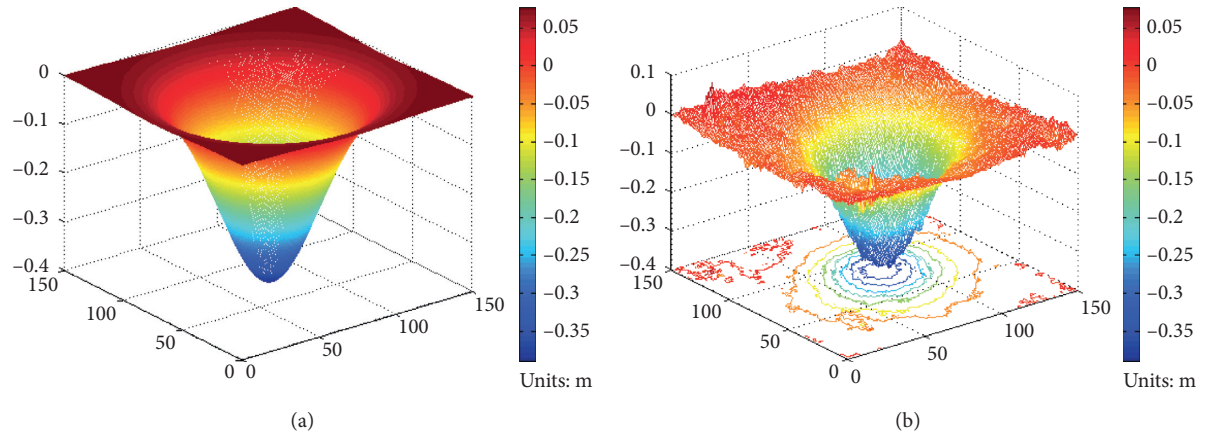

Figure 7: The 3D display of the established model in Geting Coal Mine. (a) is the 3D display of mathematical model. (b) is 3D display of the subsidence basin based on InSAR measurements.

based on the above mathematical model, quantitative analysis and simulation and early warning can be conducted on the mining settlement based on the monitoring results of InSAR.

5. Conclusions

In this paper, the land subsidence in coal mining area was monitored using InSAR technique. Using 7 scenes of L-band PALSAR data from January 2008 to February 2010, we successfully obtained the mining subsidence deformation maps in the Jining Coal Mine during different periods based on an optimum InSAR data processing flowchart and strategy.

Through this study, we got some valuable conclusions in monitoring the land subsidence in coal mining area with InSAR technique.

(1) In the Jining coalfield, some subsidence basins with the radius of tens of meters to one hundred or several hundreds were formed. Generally, the maximum deformation of the subsidence basin ranges from 30 cm to 50 cm. The land subsidence of 6 coal mines within Jining coalfield exceeds 6 km^2.

(2) The magnitude of the land subsidence in the coal mine is larger. For the larger deformation, it is easier to monitor the land subsidence using SAR interferometry with L-band data. Therefore, SAR interferometry with L-band data is an effective technique for mapping the land subsidence in mining area. In particular, SAR interferometry can detect some unknown subsidence basins.

(3) Compared with the simultaneous filed measurements, the precision of deformation measurement using D-InSAR in mining area was analyzed. The root mean square error was 1.37 cm. It can meet the needs of monitoring the mining subsidence.

(4) The method of three-dimensional mathematical modeling based on InSAR measurements is suitable for the single subsidence basin in the coal mine. The mathematical model can be used to quantitative analysis and simulation and early warning in the coal mine. In addition, for some interrupted or confused interferometric fringes caused by phase noise, the three-dimensional model of subsidence basin constructed in this paper can also be used to solve these problems, so that InSAR technology can be better applied to monitor the land subsidence in mining areas with large deformations.

When adequate SAR data are available, InSAR can partially replace the traditional leveling method for monitoring mining-induced subsidence. Therefore, InSAR technique can provide an efficient technique in monitoring the land subsidence in coal mining area.

With regard to monitoring the land subsidence in mining area, it should be noted that radar data can be used to obtain not only the quantitative ground subsidence but also the information about the land cover and the land change. In the future, we will focus on mining the surface coverage and surface changes using multitemporal SAR data.

Data Availability

The SRTM DEM data used to support the findings of this study are included within the article.

Conflicts of Interest

The authors declare no conflicts of interest.

Acknowledgments

The SRTM DEM data was provided by the National Imagery and Mapping Agency. This work was funded by the Major Science and Technology Innovation Projects of Shandong Province (2019JZZY020103). This research was supported in part by the National Natural Science Foundation of China (no. 41876202) and the Shandong Province Natural Science Foundation (no. ZR2017MD020).

References

[1] H.-d. Fan, W. Gu, Y. Qin, J.-q. Xue, and B.-q. Chen, "A model for extracting large deformation mining subsidence using D-InSAR technique and probability integral method," *Transactions of Nonferrous Metals Society of China*, vol. 24, no. 4, pp. 1242–1247, 2014.

[2] Z. Li, D. Zhang, J. Wang, Q. Zhao, and L. Pan, "Mapping land subsidence related to underground coal fires in the Wuda coalfield (northern China) using a small stack of ALOS PALSAR differential interferograms," *Remote Sensing*, vol. 5, pp. 1152–1176, 2013.

[3] L. Jiang, H. Lin, J. Ma, B. Kong, and Y. Wang, "Potential of small-baseline SAR interferometry for monitoring land subsidence related to underground coal fires: Wuda (Northern China) case study," *Remote Sensing of Environment*, vol. 115, no. 2, pp. 257–268, 2011.

[4] H. A. Zebker and R. M. Goldstein, "Topographic mapping from interferometric synthetic aperture radar observations," *Journal of Geophysical Research*, vol. 91, no. B5, pp. 4993–4999, 1986.

[5] A. K. Gabriel, R. M. Goldstein, and H. A. Zebker, "Mapping small elevation changes over large areas: differential radar interferometry," *Journal of Geophysical Research*, vol. 94, no. B7, pp. 9183–9191, 1989.

[6] R. F. Hanssen, *Radar Interferometry-Data Interpretation and Error Analysis*, Kluwer Academic Publishers, Dordrecht, The Netherlands, 2001.

[7] D. Massonnet and K. L. Feigl, "Radar interferometry and its application to changes in the earth's surface," *Reviews of Geophysics*, vol. 36, no. 4, pp. 441–500, 1998.

[8] M. Crosetto, O. Monserrat, M. Cuevas, and B. Crippa, "Spaceborne differential SAR interferometry: data analysis tools for deformation measurement," *Remote Sensing*, vol. 3, no. 2, pp. 305–318, 2011.

[9] X. Zhou, N.-B. Chang, and S. Li, "Applications of SAR interferometry in earth and environmental science research," *Sensors*, vol. 9, no. 3, pp. 1876–1912, 2009.

[10] Z. Wang, L. Liu, and X. Zhou, "Monitoring co-seismic deformation filed of Bam earthquake in Iran using D-InSAR technique," *Northwest Seismological Journal*, vol. 30, pp. 310–316, 2008.

[11] Z. Lu, T. Masterlark, and D. Dzurisin, "Interferometric synthetic aperture radar study of Okmok volcano, Alaska, 1992–2003: magma supply dynamics and post-emplacement lava flow deformation," *Journal of Geophysical Research*, vol. 110, pp. 1–18, 2005.

[12] Z. Lu, "InSAR imaging of volcanic deformation over cloud-prone areas—Aleutian islands," *Photogrammetric Engineering & Remote Sensing*, vol. 73, no. 3, pp. 245–257, 2007.

[13] L. Zhang, Z. Lu, X. Ding, H.-s. Jung, G. Feng, and C.-W. Lee, "Mapping ground surface deformation using temporarily coherent point SAR interferometry: application to Los Angeles basin," *Remote Sensing of Environment*, vol. 117, pp. 429–439, 2012.

[14] Y. Zhang, J. Zhang, W. Gong et al., "Monitoring urban subsidence based on SAR interferometric point target analysis," *Acta Geodaetica et Cartographica Sinica*, vol. 38, pp. 482–487, 2009.

[15] P. Tantianuparp, X. Shi, L. Zhang, T. Balz, and M. Liao, "Characterization of landslide deformations in three gorges area using multiple InSAR data stacks," *Remote Sensing*, vol. 5, no. 6, pp. 2704–2719, 2013.

[16] Z. Wang, J. Liu, J. Wang et al., "Resolving and analyzing landfast ice deformation by InSAR technology combined with Sentinel-1A ascending and descending orbits data," *Sensors*, vol. 20, no. 22, p. 6561, 2020.

[17] H. Fan, K. Deng, C. Ju, C. Zhu, and J. Xue, "Land subsidence monitoring by D-InSAR technique," *Mining Science and Technology (China)*, vol. 21, no. 6, pp. 869–872, 2011.

[18] M. Ji, X. Li, S. Wu, Y. Gao, and L. Ge, "Use of SAR interferometry for monitoring illegal mining activities: a case study at Xishimen iron ore mine," *Mining Science and Technology (China)*, vol. 21, no. 6, pp. 781–786, 2011.

[19] Z. Hu, L. Ge, X. Li, K. Zhang, and L. Zhang, "An underground-mining detection system based on DInSAR," *IEEE Transactions on Geoscience and Remote Sensing*, vol. 51, no. 1, pp. 615–625, 2013.

[20] M. Zheng, K. Fukuyama, and K. Sanga-Ngoie, "Application of InSAR and GIS techniques to ground subsidence assessment in the Nobi plain, Central Japan," *Sensors*, vol. 14, no. 1, pp. 492–509, 2014.

[21] A. Hayman, L. Ge, Z. Du et al., "Satellite radar interferometry for monitoring subsidence induced by longwall mining activity using Radarsat-2, Sentinel-1 and ALOS-2 data," *International Journal of Applied Earth Observation and Geoinformation*, vol. 61, pp. 92–103, 2017.

[22] Z. Yang, Z. Li, J. Zhu et al., "Locating and defining underground goaf caused by coal mining from space-borne SAR interferometry," *ISPRS Journal of Photogrammetry and Remote Sensing*, vol. 135, pp. 112–126, 2018.

[23] Y. Xia and Y. Wang, "InSAR- and PIM-based inclined goaf determination for illegal mining detection," *Remote Sensing*, vol. 12, no. 23, p. 3884, 2020.

[24] S. Du, Y. Wang, M. Zheng, D. Zhou, and Y. Xia, "Goaf locating based on InSAR and probability integration method," *Remote Sensing*, vol. 11, no. 7, p. 812, 2019.

[25] D. Chen, H. Chen, W. Zhang et al., "Characteristics of the residual surface deformation of multiple abandoned mined-out areas based on a field investigation and SBAS-InSAR: a case study in Jilin, China," *Remote Sensing*, vol. 12, no. 22, p. 3752, 2020.

[26] Z. Wang, J. Zhang, and G. Huang, "Precise monitoring and analysis of the land subsidence in Jining coal mining area based on InSAR technique," *Journal of China University of Mining and Technology*, vol. 43, pp. 169–174, 2014.

[27] X. Xu, C. Ma, D. Lian, and D. Zhao, "Inversion and analysis of mining subsidence by integrating DInSAR, Offset tracking, and PIM technology," *Journal of Sensors*, vol. 2020, Article ID 4136837, 15 pages, 2020.

[28] J. Huang, K. Deng, and H. Fan, "An improved adaptive template size pixel-tracking method for monitoring large-gradient mining subsidence," *Journal of Sensors*, vol. 2017, Article ID 3059159, 11 pages, 2017.

[29] B. Pu, C. Li, and M. Liao, "An approach for estimating underground-goaf boundaries based on combining DInSAR with a graphical method," *Journal of Sensors*, vol. 2020, 13 pages, Article ID 9375056, 2020.

[30] S. Yun, Q. Li, and X. Meng, "On time-series InSAR by SA-SVR algorithm: prediction and analysis of mining subsidence," *Journal of Sensors*, vol. 2020, Article ID 8860225, 17 pages, 2020.

[31] M. Jiang, Z. W. Li, X. L. Ding, J. J. Zhu, and G. C. Feng, "Modeling minimum and maximum detectable deformation gradients of interferometric SAR measurements," *International Journal of Applied Earth Observation and Geoinformation*, vol. 13, no. 5, pp. 766–777, 2011.

[32] Z. Wang, S. Wang, Y. Sun et al., "A new phase unwrapping algorithm based on the GVF-Snake model of edge detection," *Journal of China University of Mining and Technology*, vol. 46, no. 6, pp. 1394–1401, 2018.

[33] R. M. Goldstein and C. L. Werner, "Radar interferogram filtering for geophysical applications," *Geophysical Research Letters*, vol. 25, no. 21, pp. 4035–4038, 1998.

[34] Z. W. Li, X. L. Ding, C. Huang, J. J. Zhu, and Y. L. Chen, "Improved filtering parameter determination for the Goldstein radar interferogram filter," *ISPRS Journal of Photogrammetry and Remote Sensing*, vol. 63, no. 6, pp. 621–634, 2008.

[35] C. W. Chen and H. A. Zebker, "Phase unwrapping for large SAR interferograms: statistical segmentation and generalized network models," *IEEE Transactions on Geoscience and Remote Sensing*, vol. 40, no. 8, pp. 1709–1719, 2002.